Scanning Microscopy

Volume 7 | Number 2 Article 8

2-5-1993

Electron Acoustic Signal of Metallic Layers Over a Semiconductor Substrate

J. F. Bresse
France-Telecom

Scanning Microscopy, Vol. 7, No. 2, 1993 (Pages 523-531)
Scanning Microscopy International, Chicago (AMF O'Hare), IL 60666 USA

0891-7035/93$5.00+.00

ELECTRON ACOUSTIC SIGNAL OF METALLIC LAYERS OVER A SEMICONDUCTOR SUBSTRATE

J.F. Bresse

France-Telecom, Centre National d'Etudes des Télécommunications,Paris B
Laboratoire de Bagneux, groupement PMM, departement MPM
196 Avenue Henri Ravera, 92220 BAGNEUX - FRANCE
Phone No : 33-1-42 31 72 43
Fax No : 33-1-42 53 49 30

(Received for publication November 13, 1992, and in revised form February 5, 1993)

Abstract

Calculations have been made for the electron acoustic signal in the case of one and two metallic layers deposited over a semiconductor substrate. The temperature distribution as function of the depth has been determined by taking into account the power absorbed in the metallic layers and the substrate. We have considered strain-free and constrained layers. Experimental results have been obtained for a single metallic layer (Au, W, Pd, Mo, Mn, Ti) deposited over GaAs and for Au-Ti contacts. Comparison between experiments and calculations allows us to determine whether the layers are constrained or not.

Key Words : Scanning electron acoustic microscopy, metal, semiconductor, thin film, gold, titanium, palladium, molybdenum, manganese, tungsten, gallium arsenide, strain, thermal conductivity.

Introduction

Scanning Electron Acoustic Microscopy (SEAM) is based on the local thermal excitation of the sample and the detection of the acoustic waves generated in the heated zone due to the thermoelastic properties of the material [2][8] .

Several fields of applications have already been demonstrated for semiconductors, especially "doped area imaging in silicon" [19], as in III-V compounds [3], "crystalline lattice perturbation" after ion or proton bombardement [20] [21] and "grain boundary imaging" in silicon solar cells [1] [16]. Ohmic contacts and Schottky barriers on GaAs with interface compound formation have also been studied [3] [15] .

Visualization of non adherence zones between a metallic layer and the semiconductor is also a unique capability of this technique. Such zones have been visualized in Au and Au-Ti evaporated layers [5] [6] [15].

Selective doping by ion implantation may be visualized by a contrast in the SEAM signal. This may be correlated either to a variation of the thermal conductivity [4][6] or to a variation of the thermal expansion coefficient and other thermoelastic parameters depending on both electron-hole pairs generation and doping level [12].

SEAM Principle, Physical Phenomena

SEAM is based on a local excitation of the sample surface by a periodic electron excitation. In metals where the thermal phenomenon is the only contribution, the excitation causes a local periodic heating. The heat diffusion corresponding to this situation can be modeled by the development of a thermal wave which is damped so much that it does not propagate further than one thermal wavelength (λ_T). The solution of the diffusion equation shows that the amplitude of the thermal wave is attenuated by a factor e after a propagation of one thermal diffusion length, μ ($\mu=\lambda_T/2\pi$) expressed as :

$$\mu = \left(\frac{k'}{\pi f} \right)^{1/2} \quad \text{with} \quad k' = \frac{k}{\rho C} \qquad (1)$$

where k is the thermal conductivity, ρ the density, C the specific heat of the material, f the operating frequency and k'the thermal diffusivity.

The local heating causes a dilatation of the sample giving a stress and a strain which is relaxed through the generation of acoustic waves.

In the one-dimensional case, for a sample which is thermally thick, the temperature gradient can be approximated by [9]:

$$\theta(z) = \theta_0 \exp(-z/\mu) \qquad (2)$$

The stress-strain relation inside the sample is [20]:

$$\sigma(z) = (\lambda + 2\mu')\, \varepsilon(z) - B\, a_t\, \theta(z) \qquad (3)$$

where σ is the stress, λ the first Lamé constant, μ' the rigidity modulus, ε the strain, B the elastic bulk modulus and a_t the dilatation coefficient. These parameters are related to the sound velocity, v_s, by:

$$\lambda + 2\mu' = \rho v_S^2 \qquad (4)$$

Different types of acoustic waves have been evoked to transfer the elastic deformations through the sample, depending on the geometry of the sample, its thickness and the boundary conditions corresponding to the configuration of the sample holder for the acoustic detection.

In the case of a sample clamped by a cover and able to vibrate freely, flexural waves are the important mode of transfer of the acoustic waves to the transducer [8] [13]. This is also the case when the acoustic waves are detected by a capacitive transducer [11][12].

In our case, the sample is not clamped but glued on the tranducer which is clamped. So the sample has a good acoustic coupling with the transducer and the vibrations are transmitted through longitudinal waves, even for a thin specimen. The longitudinal acoustic wavelength, λ_a, is given by :

$$\lambda_a = v_s / f \qquad (5)$$

where v_s is the sound velocity.
In the case of a thin specimen, the sound velocity is given by :

$$v_s = \{E/\rho\}^{1/2} \qquad (6)$$

with E, Young modulus. The sound velocity is lower than the value for the bulk material.

The spatial resolution d_s is governed by the following parameters : beam spot size ϕ_b, electron range R, and the thermal diffusion length :

$$d_s = [\phi_b^2 + R^2 + \mu^2]^{1/2} \qquad (7)$$

Depending on the relative importance of these three parameters and the depth of the observed feature, one of these parameters will govern the spatial resolution.

For this study, the sample thickness is much less than the acoustic wavelength and the main contrast mechanism is not of acoustic origin. At 200 kHz, for a thin GaAs sample (i.e. 300 μm thick), the acoustic wavelength is 1.88 cm.

Signal Amplitude

The voltage signal which is detected by the transducer is in the form :

$$V(f, \phi_0) = R_{trans} \quad Re\{ S \quad e^{i\phi} \} \qquad (8)$$

where R_{trans} is the conversion factor of the transducer (V/N), Re the real part, S the amplitude of the signal, φ the phase , and ϕ_0 the offset phase of the excitation.

$$S = S_G\, S_T \qquad (9)$$

where S_G is the signal due to acoustic wave generation and S_T the acoustic wave transmission factor.

For the situation described here,we can make the following assumptions :

- the heat generation is harmonic,
- the heat generation occurs at the surface,
- the longitudinal waves are the only important mode of transfer of acoustic force from the heated zone to the transducer. In our case, the specimen thickness is less than the longitudinal wavelength giving no absorption of the acoustic waves, so $S_T = 1$.
- the characteristic length for heat transfer, or thermal diffusion length is much less than the specimen thickness.

The periodic heating of the specimen surface results in temperature gradients within the specimen. The z component of the temperature gradient can serve as a driving force for the generation of an acoustic wave.

Case of a bulk specimen

For a point source harmonic heating, the power, P, is :

$$P = P_0 e^{i\omega t} \qquad (10)$$

P_0, electron beam power, t, time, ω, angular frequency.

With the assumption that the characteristic heat transfer length is small with respect to the specimen thickness, the sample can be treated as a semi-infinite slab from the point of view of heat diffusion. Then the temperature rise distribution, θ, within the specimen is given by [9] :

$$\theta(R,t) = \frac{P_0}{2\pi k R} \exp\left[-\frac{R}{\mu}(1+i) - i\omega t \right] \qquad (11)$$

R, distance from the source.
The z component of the temperature gradient, dθ/dz is :

$$\frac{d\theta}{dz} = \frac{P_0}{2\pi k} \frac{z}{R} e^{i\omega t} \left[\frac{1+i}{\mu R} - \frac{1}{R^2} \right] \exp\left[\frac{R}{\mu}(1+i) \right] \qquad (12)$$

The equation of the motion for particle displacement is [23]:

$$\frac{\delta^2 u}{\delta z^2} + \frac{\omega}{v_S} u = \frac{B}{\rho v_S^2} a_t \frac{\delta\theta}{\delta z} \quad (13)$$

Case of specimen with a strain-free surface. The boundary condition is : $\sigma(0) = 0$.
The temperature gradient transmits its energy to the specimen through a body force [13] :

$$f = -3B a_t d\theta/dz \quad (14)$$

The temperature gradient is only significant within a distance of a few thermal diffusion lengths from the surface. As the thermal diffusion length is much less than the acoustic wavelength, the resulting force, F, is the integration of f over the specimen volume :

$$F = \iiint f \, dV \quad (15)$$

Then :

$$F = \frac{3B a_t}{(2\pi\rho f C k)^{1/2}} P_0 e^{i\omega t} e^{3i\pi/4} \quad (16)$$

so, the contribution of the acoustic wave generation to the signal is [13] :

$$S_G = \frac{3B a_t}{(2\pi f\rho C k)^{1/2}} P_0 \quad (17)$$

Case of a sample with a constrained surface. This case implies a null displacement at the surface : $u(0) = 0$
The stress inside the sample is given by [18] :

$$\sigma(z) = B a_t \bar{\theta} \quad (18)$$

$$\bar{\theta} = \frac{1}{l}\int_0^l \theta(z)dz \quad (19)$$

$$\theta(z) = \theta_0 \exp(-z/\mu_s) \quad (20)$$

$$\sigma(z) = B a_t \mu/l \theta_0 \quad (21)$$

and :

$$S_G = \pi b_1^2 B a_t \mu/l \theta_0 \quad (22)$$

where πb_1^2 is the coupling area between the transducer and the specimen.

Case of a layered sample

Two cases may be considered depending whether a strain is applied to a layer or not.
The resulting signal is the sum of the contribution of each layer and the substrate.
For a strain-free layer, we have :

$$S = \int_{z_i}^{z_{i+1}} -3(B a_t)_i \, d\theta/dz \, dz \quad (23)$$

The i^{th} layer is defined by the depth z_i and z_{i+1}, and its parameters B, a_t.
For a constrained layer, we have :

$$S = \int_{z_i}^{z_{i+1}} (B a_t)_i \theta dz \quad (24)$$

$$S = \frac{1}{l}\int_{z_i}^{z_{i+1}} (B a_t)_i \theta(z) dz \quad (25)$$

Electron energy loss and absorbed power

The interaction of the electrons with the sample gives a local heating corresponding to the electron energy loss and the absorbed power at a specific depth within the sample. Backscattered electrons which interact without energy loss with the sample do not contribute to the sample heating.

The mean energy of electrons as function of the depth, E(z), may be evaluated using an approximation of the depth-dose curve [17] :

$$\Phi(\rho z) = A_1 \exp(-a\rho z) + [B_1\rho z + \Phi(0) - A_1]\exp(-b\rho z) \quad (26)$$

$$Q = \int_0^\infty \Phi(\rho z) d\rho z = (1-k\eta) \rho (1.6 + 0.013Z) R_K \quad (27)$$

with $k = 0.45 + 0.002\,Z$
where $\Phi(\rho z)$ is the depth dose, Q the total dose, R_K the electron range, η the backscattering coefficient, ρ the density, and Z the atomic number. The parameters A_1, B_1, a, b are determined by knowing ρ, Z and R and by adjusting the two exponential functions so that they have the same slope at the junction point.
The intensity variation as a function of the depth is given by [14] :

$$I(z/R_K) = I_0 \exp\left(-\gamma \frac{z/R_K}{1 - z/R_K}\right) \quad (28)$$

with $\gamma = 0.187 \, Z^{2/3}$

and with I_0 the beam intensity.
The absorbed power below a certain depth, P(z), may be approximated by :

$$P(z) = (1-k\eta) E(z) I(z/R_K) \quad (29)$$

Surface Temperature

In order to estimate the maximum surface temperature, θ_0, we use the calculations of Wells[22] who considers the problem in three dimensions, taking into account the fact that the electron beam penetration gives an increase of both the heated depth, Z_v, and the heated surface diameter, Φ_v. The heated volume is determined by the time t_{stat}, after which the steady-state is reached.

$$t_{stat} = \frac{0.0615}{k'} \phi_v^2 \quad (30)$$

$$\phi_v^2 = \phi_b^2 + \phi_Z^2 + \phi_t^2 \quad (31)$$

$$\phi_Z = 1.117R \quad (32)$$

$$\phi_t = 2.35(k't)^{1/2} \quad (33)$$

$$Z_v^2 = \phi_Z^2 + \phi_t^2 \quad (34)$$

where Φ_b is the spot size, Φ_v the heated surface diameter, Φ_Z the interaction zone diameter, and Φ_t the diameter of the heated zone for the time to reach the steady-state.

The final maximum surface temperature is given by :

$$\theta_0 = 0.103 \frac{P_o}{k \; Z_v} \quad (35)$$

Table I gives, for several metals, semiconductors and insulators, the calculated values of ϕ_v, Zv, and θ_0 (given by Wells formula) for an electron beam of 20 keV and 100 nA, with a spot size of 0.5 µm. The electron range, used for the calculations is given by [14] :

$$R_K(\mu m) = \frac{0.276}{\rho} \frac{A}{Z^{8/9}} (E_o)^{5/3} \quad (36)$$

where A is the atomic weight, Z the atomic number and Eo the beam energy (keV).

Case of a Single Metallic Layer Over a Semiconductor Substrate

Theoretical calculations

Due to the high thermal conductivity of a metal as compared to a semiconductor, the heat diffusion maintains a constant temperature in the metal [9]. Fig.1 represents the distribution of temperature as function of the depth.

The interface temperature, θ_1, is given by the maximum increase due to the absorbed power in the metallic layer, P_{abs}^M, and the absorbed power in the substrate, P_{abs}^S :

$$\theta_1 = \frac{0.103}{(Z_v + e)} \left[\frac{P_{abs}^M}{k_M} + \frac{P_{abs}^S}{k_S} \right] \quad (37)$$

where Z_v is the heated depth in the substrate and e the thickness of the metallic layer.

For a non constrained layer, the signal is given by :

$$S = -\int_0^l 3a_t B \frac{d\theta}{dz} dz \quad (38)$$

where l is the sample thickness.

$$S = -\int_0^{z_1} (3a_t B)_M \frac{d\theta}{dz} dz - \int_{z_1}^{l} (3a_t B)_S \frac{d\theta}{dz} dz \quad (39)$$

The temperature distribution is given by :

$0 < z < z_1$, $\theta(z) = \theta_1$

$z_1 < z < l$, $\theta(z) = \theta_1 \exp(-z/\mu_S)$

The signal is expressed by :

$$S = (3a_t B)_S \; \theta_1 \quad (40)$$

For the substrate, using the same experimental conditions, the signal is given by :

$$S_S = (3a_t B)_S \theta_0^S \quad (41)$$

$$\theta_0^S = 0.103 \frac{P_0}{k_S Z_v^S} \quad (42)$$

So,

$$S/S_S = \theta_1/\theta_0^S \quad (43)$$

For a constrained layer :

$$S = \frac{1}{l} \pi b_1^2 \int_0^{z_1} (B a_t)_M \theta_1 dz - \int_{z_1}^{l} (3B a_t)_S \frac{d\theta}{dz} dz \quad (44)$$

as compared to the strain-free substrate :

$$S/S_S = \frac{e}{l} \pi b_1^2 (B a_t)_M \frac{\theta_1}{\theta_0^S} + \frac{\theta_1}{\theta_0^S} \quad (45)$$

Knowing all the parameters for the substrate and the metallic layer, the ratio S / S_S may be calculated. Table II gives the calculated values of the ratio S/S_{GaAs}, corresponding to the non constrained case, and the ratio corresponding to the constrained case, for different metallic layers on a GaAs substrate. The calculations have been made by adjusting the GaAs thermal conductivity in order to obtain a signal ratio in the non constrained case equal to the measured value. The fitted value is lower than the reported value for undoped GaAs (0.175 instead of 0.46 $W.cm^{-1}.K^{-1}$), but the substrate is a semi-insulating material with Cr incorporation to compensate for the dopant impurities, giving a reduction of the thermal conductivity. The values of thermal conductivity used for the calculations are the values given by the CRC Handbook [10].

Experiments and comparison with calculations

Different metallic layers (0.2 µm thick) have been deposited over a GaAs substrate. Au, Ti, Mn, Pd have been deposited by electron gun evaporation, W by RF sputtering and Mo by DC sputtering. Near the metallic layer, an Au layer (0.2 µm thick) has also been deposited for calibration. For each sample, two reference signals can be measured, one corresponding to the substrate and one corresponding to the Au layer.

Table I. Calculated electron range, R, heated diameter,Φ_v, heated depth, Z_v, surface temperature, θ_0, and time for steady-state, t_{stat}, using Wells expressions.

Element	R(μm)	Φ_v(μm)	Z_v(μm)	θ_0(°C)	t_{stat} (10^{-8} s)
Cu	1.45	2.18	2.12	0.20	0.26
Al	4.14	6.00	5.98	0.13	2.26
Au	0.84	1.35	1.26	0.35	0.09
Mo	1.39	2.10	2.04	0.59	0.50
Ti	2.77	4.04	4.01	2.08	12.6
W	0.84	1.36	1.27	0.65	0.17
Si	4.68	6.77	6.75	0.18	3.13
GaAs	2.54	3.71	3.67	1.00	3.52
InP	2.85	4.15	4.12	0.58	2.40
SiO_2	4.78	6.90	6.89	29.6	480
Ge	2.54	3.72	3.68	0.76	2.36

Table II Calculated values of the ratio S / S_{GaAs} (for a non constrained and a constrained layer) and experimental values for the electron acoustic signal as compared to the substrate for different metallic layers deposited on a GaAs substrate.

Metal	S/S_{GaAs} (non constrained layer)	S/S_{GaAs} (constrained layer)	S/S_{GaAs} (experiments)
Au	0.719	0.770	0.72
Ti	1.132	1.203	1.09
W	0.891	0.984	0.84
Mn	1.425	1.755	1.13
Mo	1.130	1.234	1.03
Pd	1.283	1.403	0.92

Under the same experimental conditions, the signal is measured on the GaAs substrate, the metallic layer and on the Au layer. The signal ratio of the Au layer to the GaAs substrate is used to verify the substrate homogeneity in terms of thermal conductivity.

Table II reports the experimental results obtained for a beam energy of 20 keV and an operating frequency of 200 kHz.

For most of the metals, the measured value is in good agreement with the non constrained case. For W, Mo and Pd, a better agreement should be obtained by a better estimation of the electron energy at the metal/substrate interface which governs the heated depth Z_v. A difference of 10 % of this energy may induce a difference of 17 % in the electron penetration and the heated depth. For Mn, the difference is too big to be explained only by the influence of the heated depth, but with the same energy at the interface, an agreement should be obtained with a thermal conductivity of 0.459 instead of 0.222 $W.cm^{-1}.K^{-1}$, the value given in the CRC Handbook which is only provisional[10].

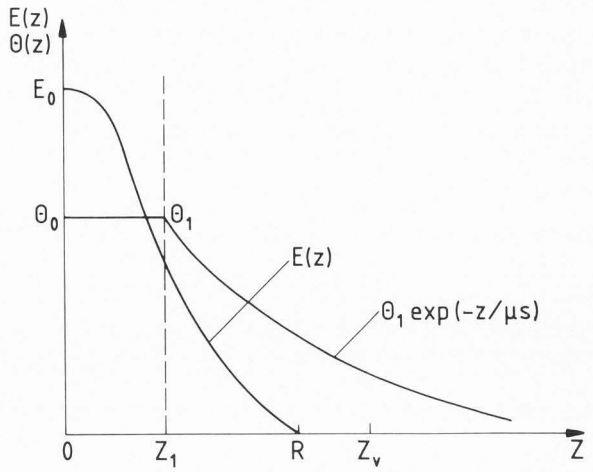

Figure 1. Temperature distribution $\theta(z)$ and electron energy E(z) in the case of a single metallic layer over a substrate.

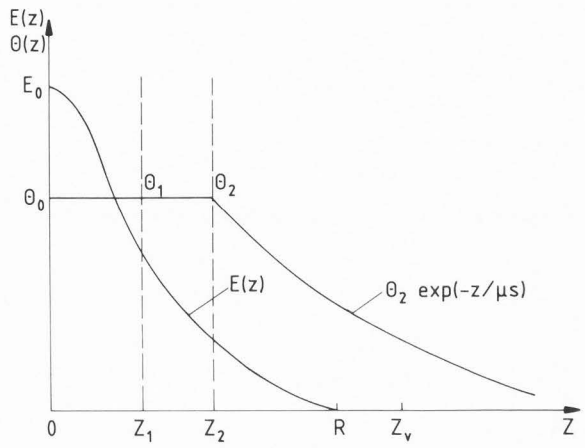

Figure 2. Temperature distribution $\theta(z)$ and electron energy E(z) in the case of two metallic layers over a substrate.

Case of Two Metallic Layers on a Semiconductor Substrate

Theoretical calculations

In analogy to the case of the single metallic layer, a constant temperature exists in the two metallic layers,

due to the high thermal conductivity of the metals as compared to the semiconductor. Fig.2 shows the repartition of temperature as function of the depth.

The interface temperature, θ_2, is given by the maximum increase due to the absorbed power in the metallic layers and in the substrate.

$$\theta_2 = \frac{0.103}{(Z_v + e_1 + e_2)} \left[\frac{P_{abs}^{M1}}{k_{M1}} + \frac{P_{abs}^{M2}}{k_{M2}} + \frac{P_{abs}^{S}}{k_S} \right] \quad (46)$$

where e_1 and e_2 are metallic layer thickness, and k_{M1} and k_{M2} the thermal conductivity of the two metals.
For the non constrained layers, the signal is given by :

$$S = -\int_0^l 3a_t B \frac{d\theta}{dz} dz \quad (47)$$

$$S = -\int_0^{z_1} (3a_t B)_{M1} \frac{d\theta}{dz} dz - \int_{z_1}^{z_2} (3a_t B)_{M2} \frac{d\theta}{dz} dz - \int_{z_2}^{l} (3a_t B)_S \frac{d\theta}{dz} dz \quad (48)$$

The temperature distribution is given by :
$0 < z < z_1$, $\theta(z) = \theta_1 = \theta_0$
$z_1 < z < z_2$, $\theta(z) = \theta_2 = \theta_0$
$z_2 < z < l$, $\theta(z) = \theta_2 \exp(-z/\mu_S)$
The signal is expressed by :

$$S = (3a_t B) \quad \theta_2 \quad (49)$$

and

$$S/S_S = \frac{\theta_2}{\theta_0^S} \quad (50)$$

For the constrained layers, several possibilities occur depending on whether one or two metallic layers are constrained.
For the upper layer constrained :

$$S = \frac{1}{l} \pi b_1^2 \int_0^{z_1} (B a_t)_{M1} \theta_2 dz - \int_{z_1}^{z_2} (3B a_t)_{M2} \frac{d\theta}{dz} dz - \int_{z_2}^{l} (3B a_t)_S \frac{d\theta}{dz} dz \quad (51)$$

as compared to the strain-free substrate :

$$S/S_S = \frac{e_1}{l} \pi b_1^2 (B a_t)_{M1} \frac{\theta_2}{\theta_0^S} + \frac{\theta_2}{\theta_0^S} \quad (52)$$

For both layers constrained :

$$S = \frac{\pi b_1^2}{l} \left[\int_0^{z_1} (B a_t)_{M1} \theta_2 dz + \int_{z_1}^{z_2} (B a_t)_{M2} \theta_2 dz \right] - \int_{z_2}^{l} (3B a_t)_S \frac{d\theta}{dz} dz \quad (53)$$

as compared to the strain-free substrate :

$$S/S_S = \pi b_1^2 \left[\frac{e_1}{l} (B a_t)_{M1} \frac{\theta_2}{\theta_0^S} + \frac{e_2}{l} (B a_t)_{M2} \frac{\theta_2}{\theta_0^S} \right] + \frac{\theta_2}{\theta_0^S} \quad (54)$$

Knowing all the parameters for the substrate and the metallic layers, the ratio S / S_S may be calculated. Table III gives the calculated values of the ratio S/S_{GaAs}, corresponding to the non constrained case and the ratio corresponding to the case of the constrained intermediate layer and the two constrained layers, for a structure Au/Ti/GaAs, with a thickness of 0.2 µm for the Au layer and a thickness of Ti varying from 5 to 50 nm. The thermal conductivity of GaAs (0.115 $W.cm^{-1}.K^{-1}$) is adjusted for the non constrained case with the ratio of the Au layer.

Experiments and Comparison with Calculations

A Ti layer (thickness varying from 5 to 50 nm) and an Au layer(0.2 µm thick) have been deposited successively by electron gun evaporation. An Au layer (0.2 µm thick) has been deposited as reference.

For the experiments, the signal is measured with the same experimental conditions on the GaAs substrate, the two metallic layers and on the Au layer taken as reference.

Table III reports the experimental results for the ratio S / S_{GaAs} obtained for a beam energy of 20 keV and an operating frequency of 200 kHz.

The evolution of this ratio is made in analogy to the case where the two layers are constrained. These results are in agreement with an improvement of the adhesion with the use of an intermediate Ti layer as found by global adherence measurements[7].

Conclusions

The electron acoustic signal has been calculated in the case of one or two metallic layers deposited on a semiconductor substrate. The effect of the strain at the surface or in the layers has been taken into account in the calculations. For different metallic layers (Au, Ti, W, Mn, Mo, Pd) deposited on GaAs, either by electron gun evaporation or sputtering, the experimental results agree with the non constrained case. For an Au/Ti/GaAs structure, the experimental results agree with the constrained case for the two layers. These results seem well correlated with the improvement of the adhesion due to the presence of an intermediate Ti layer.

Acknowledgements

The author wishes to thank C.Dubon-Chevallier and the TBH group for providing the sample.

References

[1] Balk LJ,Richard G,Kultscher N(1985). Semiconductor characterization by simultaneous evaluation of electron beam induced current and scanning electron acoustic microscopy. In Int.Phys.Conf.Ser.Nr 76 (Institute of Physics, Bristol, England), 342-349.

[2] Brandis E,Rosencwaig A(1980). Thermal wave microscopy with electron beams. Appl.Phys.Lett. 37, 98-100

Table III. Calculated values of the ratio S / S_{GaAs} (for the non constrained layers and for the constrained intermediate layer and for (the case of) both layers constrained) and the experimental values of the electron acoustic signal on a structure Au/Ti/GaAs as compared to the signal of the GaAs substrate.

	S/S_{GaAs} (non constrained layers)	S/S_{GaAs} (Ti constrained)	S/S_{GaAs} (Au / Ti constrained)	S/S_{GaAs} (experiments)
Au	0.663	-	0.710	0.665
Au-Ti (5nm)	0.656	0.657	0.703	0.705
Au-Ti (10nm)	0.653	0.655	0.701	0.715
Au-Ti (30nm)	0.652	0.658	0.704	0.720
Au-Ti (50nm)	0.658	0.668	0.714	0.733

[3] Bresse JF(1988). Scanning electron acoustic microscopy studies of III-V compounds : epitaxial layers and devices. Scanning Microscopy, 2, 813-819

[4] Bresse JF,Papadopoulo AC(1988). Evolution of the electron acoustic signal as function of doping level in III-V semiconductors. J.Appl.Phys. 64, 98-102

[5] Bresse JF(1989). Use of scanning electron acoustic microscopy for the analysis of III-V compound devices. Mater.Sci.Eng. A122, 53-56

[6] Bresse JF(1990). Use of the scanning electron acoustic microscopy(SEAM) for the study of III-V compound semiconductors. Scanning, 12, 308-314

[7] Bresse JF(1991). Etude de l'adhérence de dépots Au et Au-Ti sur GaAs. Le Vide, Les Couches Minces, Suppl. 258, 105-107

[8] Cargill III GS(1980). Ultrasonic imaging in a scanning electron microscope. Nature, 286, 691-693

[9] Carslaw HS,Jaeger JC(1973). In Conduction of heat in solids (2nd edition, Oxford University Press,London), 64-70, 255-281

[10] CRC Handbook of Chemistry and Physics(1989) (CRC Press,Inc, Boca Raton, Florida, USA), E-10

[11] Domnik M, Balk LJ(1992). Capacitive transducers for scanning electron acoustic microscopy (SEAM), Proceedings of the 19th International Symposium on Acoustic Imaging, Plenum Press, New York, 773-778.

[12] Domnik M, Balk LJ(1992). Signal generation and contrast mechanisms in electron and photoacoustic acoustic imaging of differently doped silicon, Proceedings of the 19th International Symposium on Acoustic Imaging, Plenum Press, New York, 755-759.

[13] Holstein WL(1985). Image formation in the electron thermoelastic acoustic microscopy. J.Appl.Phys. 5, 1, 2008-2021.

[14] Kanaya K, Okoyama S(1972). Penetration and energy loss theory of electrons in solid targets. J.Phys.D, 3, 43-58

[15] Kirkendall TD, Remmel TP(1984). Thermal wave imaging of GaAs material and devices. J.Physique, 45, C2, 877-880

[16] Marek J, Strausser YE(1984). Correlation of thermal wave imaging to other analysis methods. Appl.Phys.Lett.44, 1152-1154

[17] Pouchou JL(1989). Modèles de correction pour la microanalyse X quantitative. In Microanalyse par sonde électronique : aspects quantitatifs (ANRT, 101 avenue Poincaré 75016 Paris), C 1-36

[18] Rosencwaig A(1980). In Photoacoustics and photoacoustic spectroscopy (John Wiley & Sons, New York), 125-131

[19] Rosencwaig A, White RM(1981). Imaging of dopant regions in silicon with thermal wave electron microscopy. Appl.Phys.Lett. 38, 165-167

[20] Rosencwaig A(1982). Thermal wave imaging. Science, 218, 223-228

[21] Rosencwaig A(1984). Thermal wave imaging in a scanning electron microscope. Scanning Electron Microsc. 1984; IV: 1611-1628

[22] Wells OC(1965). Calculation of the heat-affected zone during pulsed electron beam machining, I.E.E.E. Trans.E.D. 12,4, 224-231

[23] White RM(1963). Generation of elastic waves by transient surface heating, J.Appl.Phys., 54, 12, 3559-3567.

Discussion with Reviewers

M.Domnik : For a typical energy dissipation volume exceeding the layer thickness, a confinement to generation at the surface only is not given. It is certainly of importance whether the metal layer is heated by the upper surface only or by additional heating via the substrate. In this manner, a dependence of the contrast on the primary beam electron energy is an inherent and unavoidable effect.

Author : For our situation, we have assumed that the heated zone due to the electron beam interaction is relatively small as compared to the thermal diffusion length. For example, in the case of an Au layer (0.2 μm thick) on GaAs, with a 20 keV beam energy, the heated depth calculated using the energy dissipation in the GaAs substrate (6.6 keV) is 0.68 μm. The total heated depth is 0.68 + 0.2 = 0.88 μm, a value which is small as compared to the thermal diffusion length of GaAs (6.2 μm at 200 kHz). Taking into account the calculations of Qian & Cantrell [24], the energy dissipation in the volume gives the same dependence of the signal, with a volume relatively small dissipation as compared to the thermal diffusion length.

M.Domnik : The precondition of Eq.5 (layer thickness less than the flexural wavelength) cannot be verified.
Author : In our case, the specimen is glued on the tranducer itself which is clamped. In this configuration, we consider that the vibrations of the sample are transmitted to the transducer. In this case, the resonance frequency is not due to the flexural vibrations of the sample but to the resonance of the transducer. Anyway, in the case of GaAs, with a Young modulus of 75.5 10^{11} dynes.cm^{-2}, a Poisson factor of 0.3, a density of 5.32 and a sample thickness of 500 µm, at a frequency of 200 kHz the flexural wavelength is 1.7 mm and the resonance frequency for a sample of dimensions 5x5 mm, 0.5 mm thick is 66 kHz. Experimentally, we do not observe any resonance frequency in this range and we have done SEAM images of the whole sample without finding patterns with nodes at a distance in the range of the flexural wavelength. This is the reason why, in our case, we assume no great absorption of the acoustic waves in the substrate and a separation of thermal and acoustic origins the SEAM signal.

M.Domnik : Where is the spatially varying energy dissipation introduced in theory and taken into account? Especially how does it influence Eq. 11?
Author : The energy dissipation is taken into account for the determination of the interface temperature metal-substrate, which is given by the dissipated power in both sides, substrate and metallic layer. That gives the repartition of temperature as a function of the depth. The temperature gradient is taken into account in Eq.11.

M.Domnik : The "heated volume" is treated as a stationary state. This is incorrect, as a stationary heat distribution will not contribute to either signal or contrast.
Author : As shown in Table I, the time of steady state in the "heated volume" is less than the pulse duration where the beam is on. Accordingly, when the beam is off, the temperature goes back to the steady state. That gives a periodic heating of the surface which gives the same temperature repartition in depth as the repartition given by the harmonic sinusoidal excitation [9].

M.Domnik : How is it possible that the two terms of Eq.39 depend on the thermal gradient $d\theta/dz$ whereas in Eq.44 only one term depends on this quantity? This is a quite controversial situation!
Author : The Eq. 44 corresponds to the case where the surface is constrained, corresponding to the equation 18 given in the reference [18].

M.Domnik : The experimental results seem to be the proof of the theory as presented (especially for Eq.39). However, one has to consider that due to an assumed constant temperature in the z direction within the metallic layer (compare Fig.1), this layer should be unable to contribute to the signal (as $d\theta/dz = 0$!). Furthermore, the results are in strong disagreement to the results of Domnik & Balk (M.Domnik & L.J.Balk(1993), Scanning Microscopy, 7, 1, Figs.16-17).
Author : The experimental results are in agreement with the theory of Eq. 39, corresponding to the non constrained case. In that case, the signal is given by the ratio of the interface temperature and the temperature of the substrate without the metallic layer. The results of Domnik & Balk do not correspond to the same case where an insulating layer has been introduced between the metallic layer and the substrate. In that case the temperature repartition should not be the same as in Fig.1 because, due to the equality of the thermal fluxes at the interface insulator-substrate, a great gradient of temperature exists in the insulating layer.

M.Domnik : Domnik & Balk [11] could demonstrate a strong frequency dependence of such surface contrasts. This effect is not considered at all in the theory of this paper. At least the consideration of a frequency dependence of the thermal diffusion length (as obvious from literature) has to be undertaken!
Author : Of course, the frequency dependence is taken into account in the value of the thermal diffusion length which gives the temperature gradient in the substrate (Fig.1). The frequency dependence is undertaken in both cases by the value of θ_S^0 which is strongly dependent on the thermal diffusion length.

F.A.Mac Donald : Have you a physical justification for the "non-constrained case" being appropriate, in the case of one deposited metallic layer?
Author : The metallic layers are deposited by different techniques (electron beam evaporation or sputtering). For this thickness (0.2 µm), the residual stress is usually very low.

F.A Mac Donald : The spatial resolution is described in Eq.7. What reference justifies this relation? How does it bear on the theoretical or experimental results presented?
Author : The SEAM spatial resolution, d_s, is defined as a rms diameter. The Eq.7 is the expression of the quadrature law for the combination of rms diameters. R and µ are taken as equal to the rms diameter of the symetrical distribution obtained by reflecting the penetration or the heated depth on the surface plane.

F.A.Mac Donald : How does the signal calculated in Eq.17, for a point source, bear on the later calculations, which are for a distributed source?
Author : At 200 kHz, the thermal diffusion length in GaAs is around 6.2 µm. At 20 keV beam energy, the electron penetration in GaAs is 2.54 µm and the heated depth is 3.67 µm, which is small as compared to μ_{GaAs}. Even when the source is distributed within the heated depth, due to non-uniform energy loss, we may approximate the distributed source as a point source.

F.A.Mac Donald : Since the sample configuration for the experimental results is not consistent with the assumption of a constrained surface, why is this calculation included (section Calculations, Sample with a constrained surface)? How can the statement immediately following Eq.21 be correct?
Author : Depending on the strain inside the deposited metallic layer, the assumption of a constrained surface may be realistic even if the sample surface is not clamped.

F.A.Mac Donald : Thermoelastic calculations for layered samples usually include continuity conditions for temperature, temperature gradient, stress, and displacement at the interface. How can the simplified treatement presented here be justified?
Author : Due to the high thermal conductivity of a metal as compared to a semiconductor, the interface condition for the temperature implies a constant temperature in the metal. The continuity of the stress and displacement is assumed, except at the surface and the bottom of the sample for the strained surface case.

F.A.Mac Donald : The signal calculations in the section Bulk Sample include an integration over the sample volume. Why does the calculations in the section Layered Sample include only an integration over z?
Author : For the calculations of a layered sample, a punctual source is considered at each depth and an integration is made over the sample volume.

F.A.Mac Donald : The calculations of Wells [22], are for a pulsed source, and assume that the temperature returns to normal between pulses. How are Wells's assumptions consistent with the conditions of the present work, in which a periodic, relatively high frequency source is used? Wells derives a pulse time, restated in the present paper in Eq.30, by a certain optimization procedure. What is the relation of the optimization conditions to those of the present work?
Author : The time for return to normal between the pulses is given by the t_{stat} value in Table I. This time is very short as compared to the pulse duration, i.e. 3.5 10^{-8} sec for GaAs as compared to a pulse duration of 2.5 µsec at 200 kHz. The time to steady-state is obtained by an iteration procedure when the heated diameter has reached the steady-state.

F.A.Mac Donald : The central result of the section Surface Temperature is Eq.35, which is used in the later sections as a basis for calculation? How does this result arise from Wells's calculations? How can the independence of the result on beam spot size be explained?
Author : The calculation is given in the Wells paper [22] (equation 42). This relation is not independent of the spot size, because the heated depth is taken for the time t_{stat}, when the steady-state is reached for the heated diameter, which depends on the value of the spot size.

F.A.Mac Donald : What is the argument which justifies the superposition used in the sections One and Two metallic layers to obtain the interface temperature?
Author : The interface temperature is given by the sum of the contributions of the thermal fluxes due to the absorbed power in each layer and in the substrate to the total heated depth.

Additional References

[24] Qian M, Cantrell JH(1989) Signal generation in Scanning Electron Acoustic Microscopy., Materials Science Engineering A122, 57-64.